Catalysis Today 139 (2008) 125–129

Contents lists available at ScienceDirect

Catalysis Today

journal homepage: www.elsevier.com/locate/cattod

Effect of preparation routes on the catalytic activity over $SmFeO_3$ oxide

Masami Mori [a], Yuji Iwamoto [a], Makiko Asamoto [a], Yoshiteru Itagaki [a], Hidenori Yahiro [a,*], Yoshihiko Sadaoka [a], Satoko Takase [b], Youichi Shimizu [b], Masayoshi Yuasa [c], Kengo Shimanoe [c], Hajime Kusaba [c], Yasutake Teraoka [c]

[a] Department of Materials Science and Biotechnology, Graduate School of Science and Engineering, Ehime University, Matsuyama 790-8577, Japan
[b] Department of Applied Chemistry, Kyushu Institute of Technology, 1-1 Sensui-cho, Tobata, City of Kitakyushu 804-8550, Japan
[c] Department of Energy and Material Sciences, Faculty of Engineering Sciences, Kyushu University, 6-1 Kasuga-koen, Kasuga-shi, Fukuoka 816-8580, Japan

ARTICLE INFO

Article history:
Available online 21 September 2008

Keywords:
Preparation of perovskite-type oxide
$SmFeO_3$
Catalytic activity
CO oxidation
XPS

ABSTRACT

The perovskite-type $SmFeO_3$ powders were prepared by the four different methods, named decomposition method of heteronuclear cyano complexes (CN), polymer precursor method (PP), reverse micelle method (RM) and reverse homogenous precipitation method (RHP), and their catalytic activities were evaluated with a CO oxidation reaction. The surface areas and the surface chemical compositions of Sm, Fe, O and C were strongly dependent on the preparation methods and calcination temperatures. On the basis of such the characteristics on the surface the factors controlling the catalytic activity are discussed.

1. Introduction

Perovskite-type oxide with basic formula ABO_3 is one of the attractive compounds among the mixed oxides used in the environmental friendly catalytic systems. Several perovskite-type oxides have been reported to show the high catalytic activity for the complete oxidation of hydrocarbons [1,2] and CO [3,4] and the decomposition of NO [5–8]. Besides the utility of perovskite-type oxide as a catalyst, several-types of perovskite-type oxides were applied to the electrochemical materials such as chemical sensors [9,10] and fuel cell electrodes [11–13].

The most significant problem for applying the perovskite-type oxide to catalytic reaction is the low surface area of perovskite-type oxide itself. One approach to overcome this problem is the usage of support with high surface area. Mizuno and co-workers [14,15] reported the supporting of $La_{0.8}Sr_{0.2}CoO_3$ on ZrO_2 by the impregnation method. The obtained perovskite-type oxide was highly dispersed on ZrO_2 and showed high catalytic activity for C_3H_8 oxidation. Some of the present authors [16] have reported that $LaMnO_3$ perovskite-type oxide was deposited inside the pore of alumina by using incipient wetness method. They demonstrated that $LaMnO_3/Al_2O_3$ gave fine particles of $LaMnO_3$, exhibiting higher activity for C_3H_8 oxidation than the bulk oxide when the activity was normalized to the weight of supported $LaMnO_3$. Similar results were reported for $LaCoO_3/CeO_2$ [17], $LaCoO_3/Ce_{1-x}Zr_xO_2$ [18,19], $LaMn_{1-y}Fe_yO_3$/carbon [20], $LaCoO_3$/mesoporous silica [21], $LaCoO_3/ZrO_2$ [22], $LaMnO_3/ZrO_2$ [23], $La_{0.7}Sr_{0.3}Mn_{0.95}Pt_{0.05}O_3$/alumina [24], $La_{0.8}Sr_{0.2}MnO_3$/metal aluminates [25,26], and the supported perovskite-type oxides cited in the review by Mizuno [27].

An alternative approach for yielding the perovskite-type oxide catalysts with high specific surface areas is to prepare the nano-sized perovskite-type oxide. In general, the specific surface area of perovskite-type oxide decreased with increasing calcination temperature. Numerous efforts for preparation techniques have been devoted to increasing the surface area of perovskite-type oxide. One of the most popular processing of perovskite-oxide powder with high surface area is sol–gel method [28]. Other processes to obtain fine particles have been also developed so far: i.e., thermal decomposition methods of organic cyano [29] and polymer precursors [30], the flame hydrolysis method of an aqueous solution of precursor salts [31], the ball-milling method [32], reverse micelle method [33], reverse homogeneous precipitation method [34] and so on.

It has been reported that the catalytic activity of perovskite-type oxide depended on the preparation methods [35]. The difference in the catalytic activity could not be explained only by the difference in the surface area. This may be ascribed to the different surface morphologies of perovskite-type oxides. In the present study, the catalytic activity of $SmFeO_3$ prepared by four

* Corresponding author. Tel.: +81 89 927 9929; fax: +81 89 927 9946.
E-mail address: hyahiro@eng.ehime-u.ac.jp (H. Yahiro).

0920-5861/$ – see front matter © 2008 Elsevier B.V. All rights reserved.
doi:10.1016/j.cattod.2008.08.014

different methods: the thermal decomposition methods of the organic heteronuclear cyano metal complex (abbreviated as CN method) and polymer precursor including metal ions (PP method), and the calcination of hydroxides of heterometals synthesized by reverse micelle method (RM method) and reverse homogeneous precipitation method (RHP method), were compared each other and the factor controlling the catalytic activity of $SmFeO_3$ was discussed on the basis of XPS results.

2. Experimental

2.1. Sample preparation

2.1.1. Decomposition method of heteronuclear cyano complexes (CN) [29]

The heteronuclear cyano complexe, $Sm[Fe(CN)_6]\cdot nH_2O$, as a precursor of perovskite-type oxide was synthesized at room temperature by mixing aqueous solutions of appropriate amounts of $Sm(NO_3)_3H_2O$ and $K_3Fe(CN)_6$ under continuous stirring, according to the following reaction; $SmNO_3(aq) + K_3Fe(CN)_6(aq) \rightarrow SmFe(CN)_6\cdot nH_2O(s) + 3KNO_3(aq)$. The precipitate obtained was collected by suction filtration, washed with deionized water, ethanol, and diethyl ether, and then dried in air at 50 °C. The resulting powder was calcined at 550–800 °C for 5 h in air.

2.1.2. Decomposition method of polymer precursor method (PP) [30]

$Sm(NO_3)_3$ and $Fe(NO_3)_3$ were dissolved in an ethylene glycol solution at the desired metal molar ratio. Acetylacetone (acac) was then added (oxide:acac = 1 mol:8 mol) as a chelating agent, and next a polymer, i.e., poly(vinyl alcohol) (PVA) or poly(ethylene glycol) (PEG) was added as the polymer additive (7.5 wt%) to form the polymer precursor. The prepared polymer precursor was decomposed on a heating-plate to obtain the powders. The powders were calcined at 550–800 °C for 2 h.

2.1.3. Reverse micelle method (RM) [33]

Two kinds of reverse micelle solutions (RM solutions A and B) were prepared by using hexaethyleneglycol nonylphenyl ether (NP-6) and cyclohexane, surfactant and solvent, respectively. RM solution A (RM-A) contained an aqueous solution of an equimolar mixture of $Sm(NO_3)_3$ and $Fe(NO_3)_3$ (0.2 M), while RM solution B (RM-B) contained an aqueous solution of tetramethylammonium hydroxide (TMAH, 10 wt%, coprecipitator). The ratio of water to surfactant was set in 9 in both solutions. When RM-A was poured into RM-B under agitation by stirring, a yellow colored transparent solution, which could be an RM solution including mixed hydroxides of Sm^{3+} and Fe^{3+}, was obtained. After stirring for 1 h, ethanol was added to the solution to collect the hydroxide precursor by breaking reverse micelles. After filtration and drying, obtained precursor was calcined in air in the range of 550–800 °C.

2.1.4. Reverse homogenous precipitation method (RHP) [34]

Samarium and iron nitrates (0.02 mol for each) were dissolved in 100 mL of deionized water. The mixed nitrate solution was then dropped through a burette at a rate of 0.5–1.0 mL min^{-1} into aq. NH_3 (300 mL, pH 13) under vigorous stirring. The final pH of the reaction medium was about 11. The suspension was further stirred for 1 h, kept standing for 30 min, and filtrated to collect the solid precursor (hydroxide). The precursor was dried at 110 °C for 12 h, and calcined at 550–800 °C in air.

2.2. Characterization and catalytic reaction of $SmFeO_3$

The crystalline structure of the products was elucidated using the powder XRD (Rint 2000, Rigaku, Cu K_α) and the surface areas of the obtained powders were determined with the BET analysis for the adsorption–desorption property measurements (Belsorp-mini, BEL Japan) using N_2 adsorbent at 77 K. The surface chemical states and compositions of the $SmFeO_3$ oxides were evaluated by X-ray photoelectron spectroscopy (XPS) analyses (XPS 1600E, PerkinElmer) using an Mg K_α excitation sources. All the binding energy (BE) values were referenced to the C 1s line at 284.5 eV. The sputtering was conducted with argon gas. The thermal desorption profile was measured with quadrupole mass spectrometer (JEOL SUN200) attached with thermogravimetric analyzer (Seiko Instruments Inc., TG/DTA6200).

The catalytic reaction of CO oxidation was carried out in a conventional fixed-bed flow reactor. The perovskite-type oxide catalyst (0.5 g) was placed in the flow reactor. The reaction gas contained 1.0 vol% of CO, 20.0 vol% of O_2, and helium as a balance gas. The total flow rate was 50 cm^3 min^{-1}. The reaction temperature was increased stepwise from 100 to 400 °C, and the reaction was carried out at each temperature until the conversion reached a constant value. The gas composition was analyzed by gas chromatography (Shimazu, GC-8AIT) using molecular sieve 5 A and active carbon columns. The activity was evaluated by the conversion of CO ($([CO]_{out}/[CO]_{in}) \times 100\%$).

3. Results and discussion

Fig. 1 shows the XRD profiles of $SmFeO_3$ prepared by different methods. The calcination temperature was unified to 700 °C. The samples prepared by the CN, RM, and RHP methods provided the XRD patterns indicating the single phase formation of the perovskite-type structure of $SmFeO_3$ (JCPDS# = 82424). The XRD profile of the sample prepared by the PP method contains a weak signal at 28.3 degree assigned to the impurity of Sm_2O_3, although the relative intensity of this impurity signal normalized by the (1 2 1) signal is ca. 0.08. Except for the impurity signals, any outstanding differences (peak position, line-width, etc.) were not confirmed in the XRD patterns.

Fig. 2 shows the change in the BET surface areas of the $SmFeO_3$ powders with calcination temperatures. For all the methods, the surface areas were decreased with the increase in calcination temperature. For the RM method, for example, the value at 600 °C was around 20 m^2 g^{-1} and this is 5 times higher than that at the 800 °C calcination. The surface area seems to depend on the preparation methods as well. Although the difference is not remarkable, the CN and PP methods gave the trend of lower surface areas compared to the RM and RHP methods.

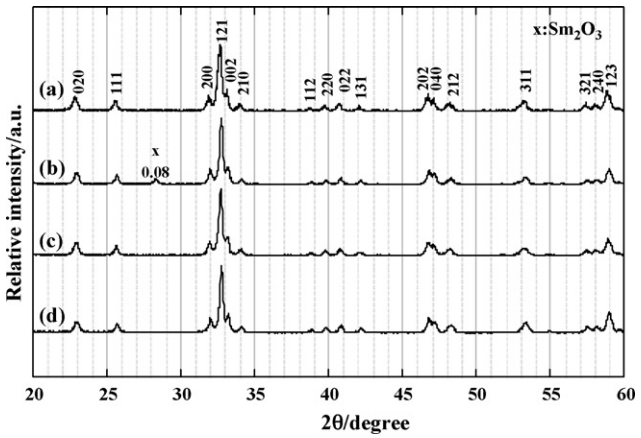

Fig. 1. XRD profiles of $SmFeO_3$ prepared by (a) CN, (b) PP, (c) RM, and (d) RHP methods. The samples were calcinated at 700 °C.

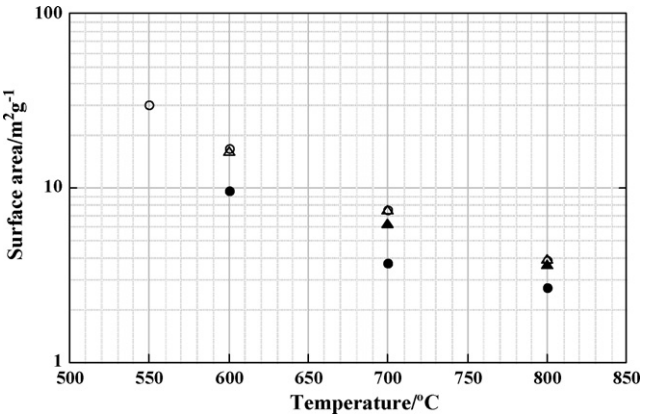

Fig. 2. Surface area changes with the calcination temperatures: (●) CN, (▲) PP, (○) RM, and (△) RHP methods.

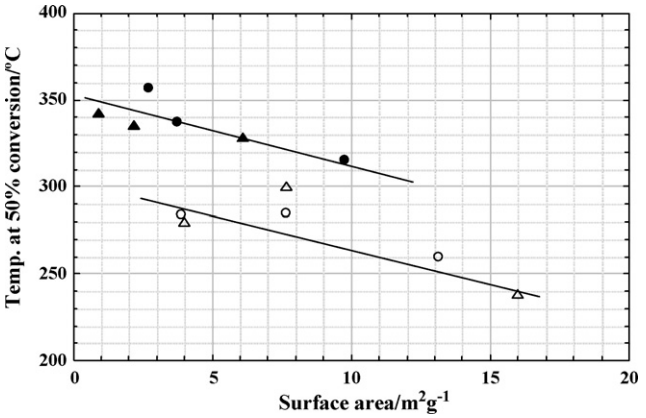

Fig. 3. The catalytic activity for CO oxidation of $SmFeO_3$ as a function of surface area: (●) CN, (▲) PP, (○) RM, and (△) RHP methods.

The catalytic activities of each $SmFeO_3$ powder were characterized by examining a CO oxidation reaction. Fig. 3 demonstrates how the surface area affects the catalytic activity. Two groups of linear relationships were found between the BET surface area and the temperature for the 50% CO conversion (as an index of the catalytic activity), and such a temperature was reasonably reduced with an increase in the surface area. One group consists of the powders prepared by the CN and PP methods and the other consists of the powders prepared by the RM and RHP methods. The former group was lower in the activity than the latter. Overall, the difference of the temperature between the two groups is around 50 °C. Since the difference in the surface area is not large, only the BET surface area cannot explain the difference in the catalytic activity. Therefore, not only a surface area but also a surface chemical composition of the $SmFeO_3$ oxides would also be an important factor as discussed later.

It is possible that the surface composition of the $SmFeO_3$ oxides, Sm, Fe, lattice and adsorbed oxygen can be a controlling factor for the catalytic activity of the CO oxidation reaction. For this reason, the XPS analyses targeting at surface O, Sm and Fe elements were carried out. Fig. 4 shows the O 1s XPS peaks for the $SmFeO_3$ prepared by the CN method recorded before and after the sputtering. The O 1s peaks can be deconvoluted into two components: one component at lower BE is attributable to the lattice oxygen ($O_{lattice}$) and the other at higher BE is to the surface adsorbed oxygen (O_{ad}). The BE of $O_{lattice}$ (529.0 eV) is intermediate between those of Sm_2O_3 (528.6 eV) and Fe_2O_3 (529.6 eV) [36]. Before the sputtering, the two oxygen species were observed with

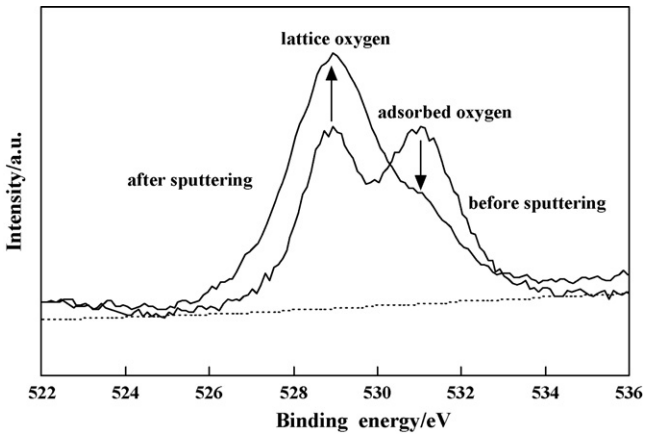

Fig. 4. O 1s XPS spectra of $SmFeO_3$ prepared by the CN method at calcinations temperature of 700 °C.

almost equal intensity. By the sputtering, the surface adsorbed oxygen notably reduced concomitantly with an increase in the intensity of the lattice oxygen. This is clearly due to that the surface oxygen was eliminated during the sputtering process and, at the same time, the lattice oxygen emerged at the surface. As mentioned later, carbonate species exists on the surface of the oxides; therefore the detected O_{ad} element might be ascribed to the oxygen in the carbonates.

Fig. 5 shows the correlation between the amounts of O/Sm ($O_{lattice}$/Sm and O_{ad}/Sm) and Fe/Sm derived from the result of the XPS analyses for the different preparation methods and calcination

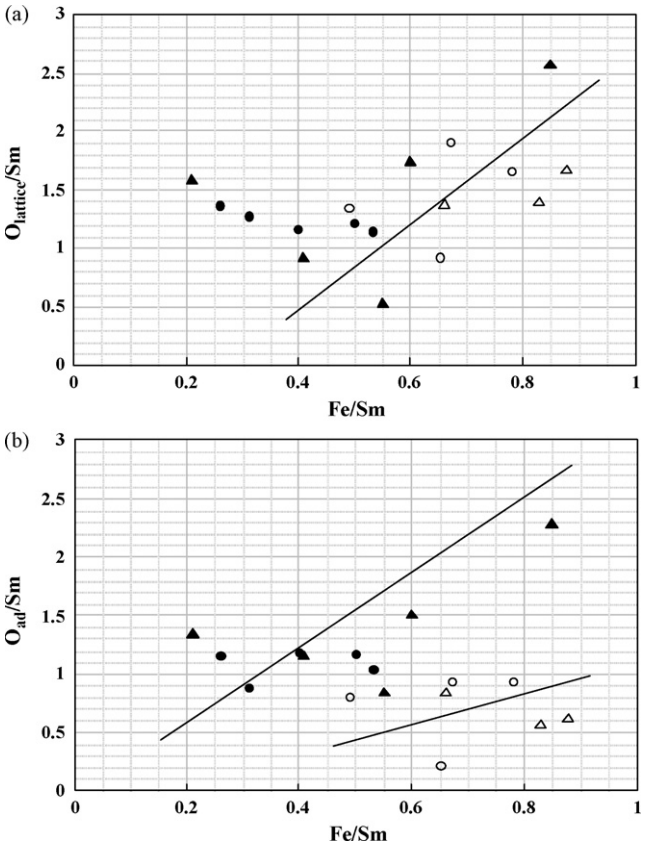

Fig. 5. Correlations of the surface chemical compositions between (a) $O_{lattice}$/Sm and Fe/Sm and (b) O_{ad}/Sm and Fe/Sm for the sample prepared with the different methods and calcination temperatures: (●) CN, (▲) PP, (○) RM, and (△) RHP methods.

temperatures. In all the samples, the ratios of Fe/Sm were <1, indicating that they possess Sm-enriched surfaces especially in the CN and PP methods. In the region of Fe/Sm <0.4, the value of $O_{lattice}$/Sm falls on 1.2–1.5, suggesting that the surfaces are more in Sm_2O_3-like features. The value of $O_{lattice}$/Sm shifted to increase linearly at above 0.4 and became close to 3 when the value of Fe/Sm is close to 1 (which is the stoichiometric ratio of Sm, Fe and O in the perovskite structure). The amount of O_{ad} also seems to increase with an increase in that of Fe/Sm. This might indicate that O_{ad} species adsorbs more favorably on the Fe sites rather than the Sm sites.

The correlation between the surface concentrations of $O_{lattice}$ and O_{ad} are shown in Fig. 6. Linear relationships were clearly found between the two oxygen species; the O_{ad} increased with an increase in the $O_{lattice}$. The relationships were again grouped into two groups: one is the CN and PP methods and the other is the RM and RHP methods. The surface of the former group is more abundant in O_{ad} than that of the latter group. Given the catalytic activity of the latter group was superior to the former (Fig. 3), it is thus possible that the O_{ad} species on the Fe surface reduces the catalytic activity. In turn, this result supports that the Fe site or B site is an active site for the CO oxidation.

The formation of carbonate species is known for the oxides prepared via organic precursors [28,34]. The carbonate species exists on the surface of the catalysts possibly related to the catalytic activity. Therefore, the XPS analysis was also conducted for C 1s spectra. Fig. 7 shows the C 1s XPS spectra of the samples prepared from the four different methods. These spectra were collected before sputtering. The peaks at 284.5 eV are those of the referenced contaminated carbon. The carbonate peaks were weakly observed at higher BE and their relative intensities to the carbon reference are fairly dependent on the preparation methods in the order of PP > CN >> RHP > RM. Fig. 8 shows the correlation between the amounts of C/Sm and Fe/Sm. Two kinds of linear relationships were suggested, one was grouped by the RHP and RM methods and the other was by the CN and PP methods. In both the groups, the C/Sm values increased with an increase in Fe/Sm. In particular, the dependence of the latter group is more prominent than that of the former. This indicates that Fe is likely to be a dominant adsorption site of the carbonates. The methods in the latter group are possibly in a more favorable environment for the formation of the carbonate species. In both the groups, higher values of C/Sm and Fe/Sm are realized at higher calcination temperature. Although the reason is still unclear, the PP powder cacinated at 600 °C (denoted as PP-600) seems to contain distinctly large amount of carbonate species.

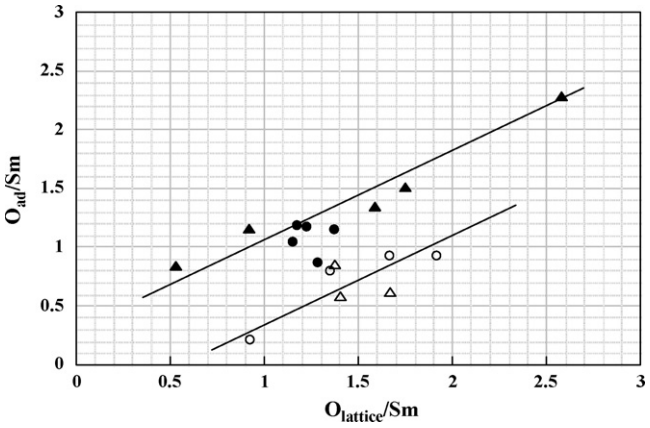

Fig. 6. Correlation between $O_{lattice}$/Sm and O_{ad}/Sm on the surfaces: (●) CN, (▲) PP, (○) RM, and (△) RHP methods.

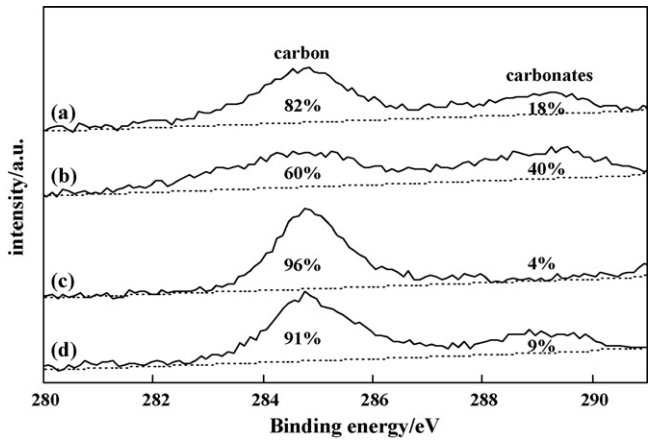

Fig. 7. C 1s XPS spectra of the $SmFeO_3$ prepared by (a) CN, (b) PP, (c) RM, and (d) RHP methods, where the samples were prepared at 700 °C. The relative intensities of the C 1s peaks in % are denoted in the figure.

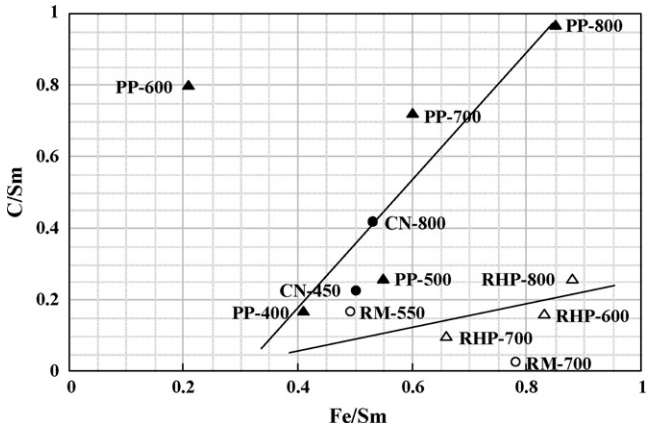

Fig. 8. Correlation of the surface compositions between C/Sm and Fe/Sm: (●) CN, (▲) PP, (○) RM, and (△) RHP methods.

Fig. 9 shows the results of the thermal desorption MS spectroscopy of CO_2 (m/e = 44) released from the $SmFeO_3$ oxides prepared at 700 °C, where the intensities are calculated as those per unit weight and surface area. Desorption peaks were observed in the three temperature regions, around 100, 250, and 500 °C. The

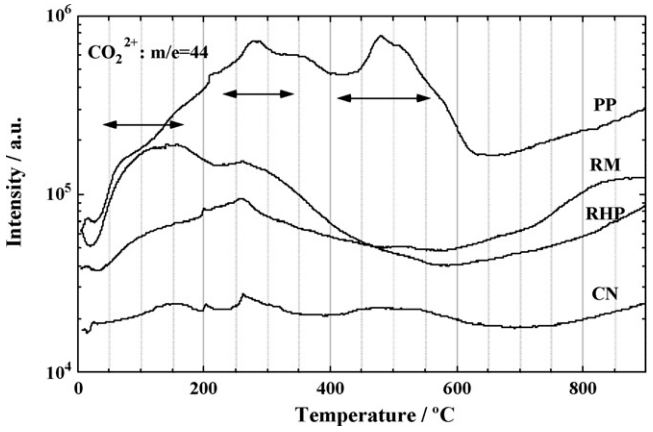

Fig. 9. Thermal desorption profiles of CO_2 measured for the $SmFeO_3$ powders detected by MS (m/e = 44 [CO_2^+]), where the samples were prepared at 700 °C. The relative intensity was defined as total ion count of [CO_2^+] per unit weight and surface area.

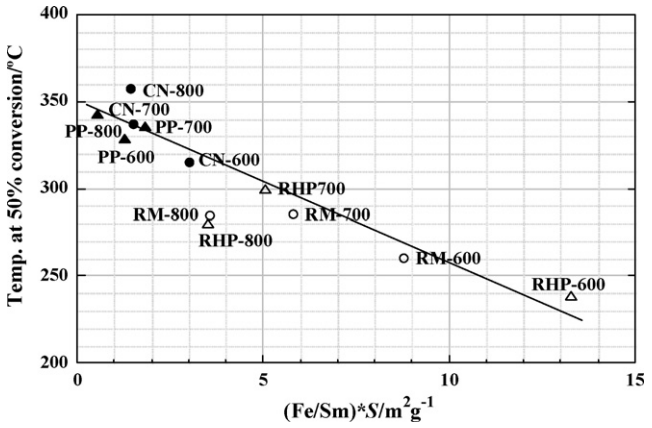

Fig. 10. The catalytic activities of the $SmFeO_3$ for CO oxidation as a function of multiplication product of Fe/Sm and surface area (*S*), (Fe/Sm)*S*.

first two peaks were observed for all the samples, probably being originated from weakly bound CO_2 species on the oxide surfaces. However, the third peaks were seen only in the PP and CN samples. In particular, peak intensities in the PP sample were significantly higher than those in the others. The order of intensities accommodates to the XPS result in which the CN and PP methods give a higher peak intensities of the carbonates compared to the RM and RHP methods. It seems that the order of the third peaks is compatible with the result of the C 2s XPS in Fig. 7. Therefore the third peaks are attributable to strongly bound carbonate species. As shown in Fig. 3, the activities of the oxides prepared at 700 °C are classified into two groups; CN- and PP-700 as a lower activity and RHP- and RM-700 as higher activity. The oxides prepared by the former methods contain the carbonate species observed as third peaks in the MS spectra absorbed on the active site of the oxides. Thus it was clarified that the surface chemical compositions as well as the surface areas could control the catalytic activity. Since the CO_2 species corresponding to the first and second peaks are released at the reaction temperature, they have small or no contributions to the catalytic activities.

Fig. 10 finally summarizes the correlation between the catalytic activity and the multiplied product of Fe/Sm and the surface areas. The single linear relationship was clearly confirmed. Fig. 10 demonstrated that the surface concentration of Fe is the main factor of catalytic activity and Fe acts as a catalytically active site for CO oxidation. The higher activities were achieved with the RM and RHP method, especially at the lower calcination temperatures.

4. Conclusion

The perovskite-type $SmFeO_3$ oxides were prepared by the four different methods (CN, PP, RM and RHP). Except the precursor prepared by the PP-method, calcination of precursors at 550–800 °C gave single $SmFeO_3$ oxide phases. The surface areas and the surface elemental compositions were dependent on the methods and calcination temperatures. The difference of such the characteristics of the powders reflected in the catalytic activity for the CO oxidation. The BET surface area analysis indicated that the RM and RHP methods gave slightly higher surface areas than the other methods. The XPS and thermal desorption MS analyses on the surface concentrations of O_{ad}, $O_{lattice}$, Sm, Fe and C gave following knowledge. (1) The O_{ad} species were probably originated from the carbonate species and preferably adsorbed on the Fe sites, which reduced the number of active sites on the surface. (2) The surface of RM and RHP have larger amount of Fe than that of CN and PP. From the above analyses, the particles prepared by the RM and RHP methods have better surfaces for their higher catalytic activities. This effect is more prominent at lower calcination temperatures. It is thus concluded that both surface area and surface chemical composition are the factors controlling the catalytic activity and these factors strongly related to the preparation method and calcination temperature.

Acknowledgement

This work was financially supported by the Core Research for Evolutional Science and Technology (CREST) program of the Japan Science and Technology Agency (JST).

References

[1] T. Nakamura, M. Misono, T. Uchijima, Y. Yoneda, Nippon Kagaku Kaishi (1980) 1679.
[2] T. Nitadori, T. Ichiki, M. Misono, Bull. Chem. Soc. Jpn. 61 (1988) 621.
[3] P.K. Gallagher, D.W. Johnson Jr., E.M. Vogel, J. Am. Ceram. Soc. 60 (1977) 28.
[4] N. Mizuno, Y. Fujiwara, M. Misono, J. Chem. Soc., Chem. Commun. (1989) 316.
[5] J. Wang, H. Yasuda, K. Inumaru, M. Misono, Bull. Chem. Soc. Jpn. 68 (1995) 1226.
[6] Z. Zhao, X. Yang, Y. Wu, Appl. Catal. B 8 (1996) 281.
[7] Y. Teraoka, T. Harada, S. Kagawa, J. Chem. Soc., Faraday Trans. (1998) 1887.
[8] T. Ishihara, K. Anami, K. Takiishi, H. Yamada, H. Nishiguchi, Y. Takita, J. Catal. 220 (2003) 104.
[9] H. Aono, E. Traversa, M. Sakamoto, Y. Sadaoka, Sens. Actuators B 94 (2003) 132.
[10] N.N. Toan, S. Saukko, V. Lantto, Physica B: Condens. Matter 327 (2003) 279.
[11] J. Mizusaki, Solid State Ionics 52 (1992) 79.
[12] H.Y. Tu, Y. Takeda, N. Imanishi, O. Yamamoto, Solid State Ionics 117 (1999) 277.
[13] H. Yahiro, H. Yamaura, M. Asamoto, Mater. Res. Soc. Symp. Proc. 927 (2007) 21.
[14] H. Fujii, N. Mizuno, M. Misono, Chem. Lett. (1987) 2147.
[15] N. Mizuno, H. Fujii, H. Igarashi, M. Misono, J. Am. Chem. Soc. 114 (1992) 7151.
[16] H. Kusaba, T. Asada, T. Kayama, K. Sasaki, Y. Teraoka, Shokubai 47 (2005) 171.
[17] M. Alifanti, M. Florea, V. Cortes-Corberan, U. Endruschat, B. Delmon, V.I. Pârvulescu, Catal. Today 112 (2006) 169.
[18] M. Alifanti, N. Blangenois, M. Florea, B. Delmon, Appl. Catal. A 280 (2005) 255.
[19] M. Alifanti, M. Florea, V.I. Pârvulescu, Appl. Catal. B 70 (2007) 400.
[20] S. Imaizumi, K. Shimanoe, Y. Teraoka, N. Miura, N. Yamazoe, J. Electrochem. Soc. 151 (2004) A1559.
[21] S.V. Nguyen, V. Szabo, D. TrongOn, S. Kaliaquine, Micropor. Mesopor. Mater. 54 (2002) 51.
[22] S. Colonna, S. De Rossi, M. Faticanti, I. Pettiti, P. Porta, J. Mol. Catal. A 180 (2002) 161.
[23] S. Cimino, S. Colonna, S. De Rossi, M. Faticanti, L. Lisi, I. Pettiti, P. Porta, J. Catal. 205 (2002) 309.
[24] N.K. Labhsetwar, A. Watanabe, R.B. Biniwale, R. Kumar, T. Mitsuhashi, Appl. Catal. B 33 (2001) 165.
[25] R. Burch, P.J.F. Harris, C. Pipe, Appl. Catal. A 210 (2001) 63.
[26] P.E. Marti, M. Maciejewski, A. Baiker, Appl. Catal. B 4 (1994) 225.
[27] N. Mizuno, Catal. Today 8 (1990) 221.
[28] H.M. Zhang, Y. Teraoka, N. Yamazoe, Chem. Lett. (1987) 665.
[29] Y. Sadaoka, E. Traversa, M. Sakamoto, J. Alloys Compd. 240 (1996) 51.
[30] K. Tsuchida, S. Takase, Y. Shimizu, Sens. Mater. 16 (2004) 171.
[31] I. Rossetti, L. Forni, Appl. Catal. B 33 (2001) 345.
[32] V. Szabo, M. Bassir, A. VanNeste, S. Kaliaguine, Appl. Catal. B 37 (2002) 175.
[33] M. Yuasa, K. Shimanoe, Y. Teraoka, N. Yamazoe, Catal. Today 126 (2007) 313.
[34] Y. Teraoka, S. Nanri, I. Moriguchi, S. Kagawa, K. Shimanoe, N. Yamazoe, Chem. Lett. 29 (2000) 1202.
[35] E. Campagnoli, A. Trvares, L. Fabbrini, I. Rossetti, Yu.A. Dubitsky, A. Zaopo, L. Forni, Appl. Catal. B 55 (2005) 133.
[36] H. Aono, M. Sato, E. Traversa, M. Sakamoto, Y. Sadaoka, J. Am. Chem. Soc. 84 (2001) 341.